CoTaZr/Pd multilayer with perpendicular magnetic anisotropy

Yong Chang Lau, Hüseyin Kurt, and J. M. D. Coey

Citation: APL Materials **1**, 022104 (2013); doi: 10.1063/1.4818004
View online: http://dx.doi.org/10.1063/1.4818004
View Table of Contents: http://scitation.aip.org/content/aip/journal/aplmater/1/2?ver=pdfcov
Published by the AIP Publishing

CoTaZr/Pd multilayer with perpendicular magnetic anisotropy

Yong Chang Lau,[a] Hüseyin Kurt,[b] and J. M. D. Coey
School of Physics and CRANN, Trinity College, Dublin 2, Ireland

(Received 2 March 2013; accepted 17 May 2013; published online 12 August 2013)

We report a novel perpendicularly magnetized thin film $[Co_{91.5}Ta_{4.5}Zr_4/Pd]_5$ multilayer, which exhibits strong perpendicular magnetic anisotropy when grown on 5 nm of Pd and Ru seed layers. The Pd-seeded multilayer annealed at 300 °C shows an effective uniaxial anisotropy constant, $K_{eff} = 1.1$ MJ m^{-3}, with an anisotropy field as high as 1.6 T. The perpendicular anisotropy is sustained on annealing at 400 °C for 1 h. X-ray diffraction on multilayers with 30 repeats suggests that the use of amorphous CoTaZr reduces the stress of the stack, compared to [Co/Pd] multilayer. [http://dx.doi.org/10.1063/1.4818004]

Recently, multilayer thin films with perpendicular magnetic anisotropy (PMA)[1] have attracted much interest as they are potentially valuable in various applications, ranging from ultrahigh density bit-patterned media[2] to magnetic-tunnel-junction-based magnetic random access memory (MRAM).[3–6] A number of multilayer systems, where typically ultrathin Co or cobalt-based alloy layers of a few tenths of nanometer in thickness are sandwiched between fcc(111) oriented transition metal layers such as Pd,[7] Pt,[8] Ni,[9] and Au,[10] are known to exhibit PMA. Magnetic properties of a multilayer can be tuned easily by varying the thickness of individual layer, the number of repeats, the seed layer, the deposition conditions, or the post thermal annealing temperature.[11–16] This allows the material properties to be engineered to suit a given application. In this letter, we present $[Co_{91.5}Ta_{4.5}Zr_4/Pd]$ multilayer system, which exhibits strong out-of-plane anisotropy with the effective perpendicular anisotropy constant, K_{eff}, as high as 1.1 MJ m^{-3} after annealing at 300 °C. In addition, the multilayer shows high thermal annealing stability, retaining strong PMA upon annealing at 400 °C for 1 h. The system could be a candidate for applications in magnetic storage devices.

Amorphous $Co_{91.5}Ta_{4.5}Zr_4$ is a soft ferromagnet with high saturation magnetization, $M_s = 1.2$ MA m^{-1}, low coercivity, $\mu_0 H_c < 1$ mT, high thermal annealing stability up to $T_a = 400$ °C, and high resistivity, $\rho \sim 100\ \mu\Omega$ cm.[17] The 4.5% of Ta significantly reduces the magnetostriction of the material compared to bulk Co, and 4% of Zr helps to make the alloy amorphous. Previously, CoTaZr has been used as a soft magnetic underlayer in CoCrPt-based recording media and in magnetic recording heads.[18,19] The CoTaZr alloy is also interesting for on-chip inductor cores because the high relative permeability of the alloy increases the inductance, while the high resistivity reduces the eddy current loss.[17,20]

Here, we grew [CoTaZr/Pd] multilayer stacks on thermally oxidized Si(100) substrates at ambient temperature by dc magnetron sputtering in an automated Shamrock deposition tool with a base pressure better than 2×10^{-7} Torr. A typical stack structure consists of Si/SiO_2 substrate/seed layer/$[CoTaZr(t)/Pd(0.5)]_5$/Ta(2) (thicknesses in nanometres) with 0.2 nm $< t <$ 0.5 nm. The deposition rates of CoTaZr and Pd were 0.010 nm/s and 0.024 nm/s, respectively. Samples were annealed

[a]Author to whom correspondence should be addressed. Electronic mail: lauyc@tcd.ie
[b]Present address: Engineering Physics Department, Istanbul Medeniyet University, Göztepe Kadıköy, Istanbul, Turkey.

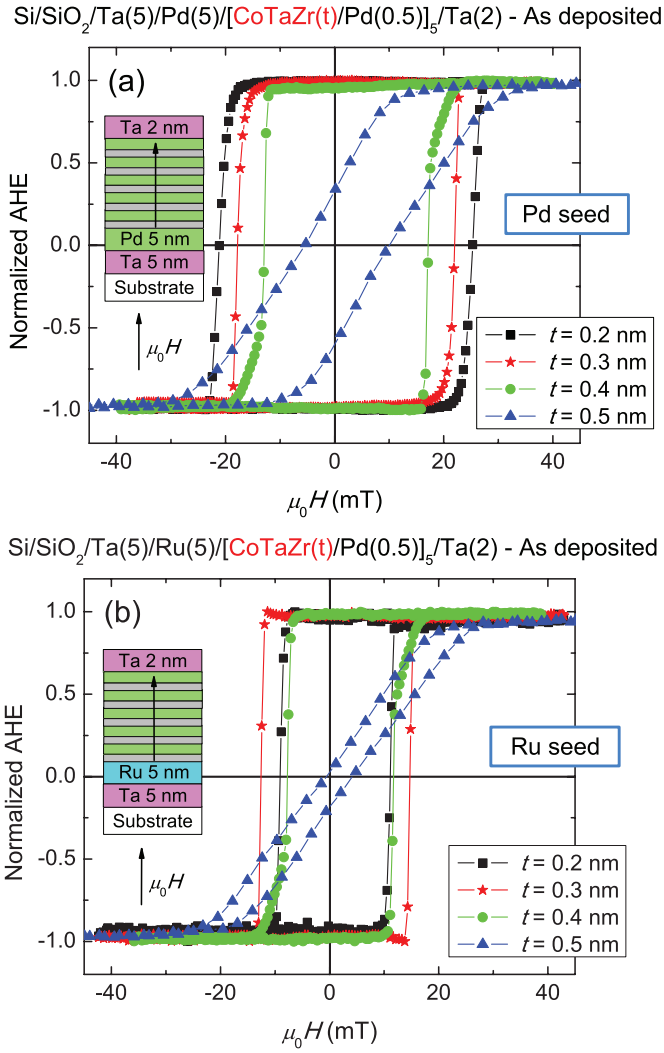

FIG. 1. Normalized AHE loops of as-deposited $[CoTaZr/Pd]_5$ multilayers grown on (a) 5 nm of Pd, and (b) 5 nm of Ru seed layers.

at temperatures ranging from 300 °C to 400 °C in high vacuum under a perpendicular magnetic field of 0.8 T. Anomalous Hall Effect (AHE) responses were measured in the standard four point configuration within an electromagnet capable of generating out-of-plane fields up to 180 mT. Magnetization for both in-plane and out-of-plane configurations was measured on 4 mm square samples in a Quantum Design superconducting quantum interference device (SQUID) magnetometer. Grazing incidence X-ray reflectivity and X-ray diffraction were carried out in a Bruker D8 diffractometer with a monochromated Cu-K_α source.

We first investigate the effect of the seed layer on the magnetic properties of the [CoTaZr/Pd] multilayers. Three series of samples were prepared on different seed layers: Ta(5), Ta(5)/Pd(5), and Ta(5)/Ru(5). X-ray diffraction on samples with thicker seed layer only (Ta(5)/X(15); X = Ta, Pd, or Ru) reveals their crystalline nature, with diffraction peaks corresponding to tetragonal β-Ta (002), fccPd (111), and hexagonal Ru (0002), respectively. Figure 1 shows the normalized AHE loops of as-deposited [CoTaZr(t)/Pd(0.5)] multilayers grown on Ta(5)/Pd(5) and Ta(5)/Ru(5) buffer layers with the field applied normal to the film plane. t varies from 0.2 nm to 0.5 nm in steps of 0.1 nm. The individual Pd layer thickness and the number of multilayer repeats are fixed at 0.5 nm and 5, respectively. For t = 0.2–0.4 nm, Pd-seeded and Ru-seeded multilayer stacks show square hysteresis loops with sharp switching at a coercive field, $\mu_0 H_c$ of approximately 30 mT and 10 mT,

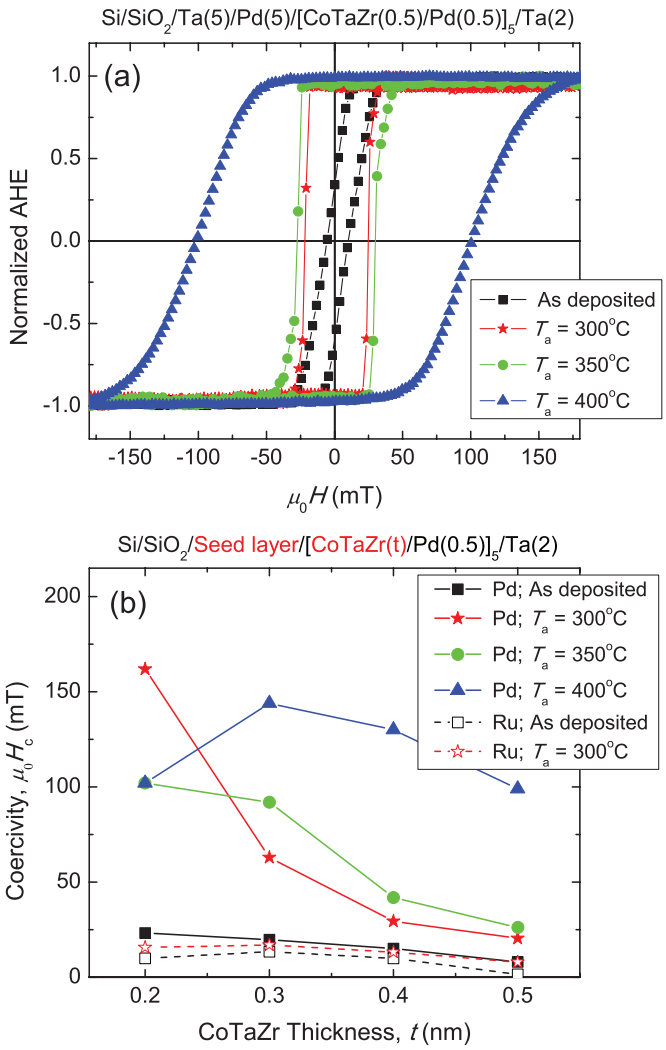

FIG. 2. (a) Normalized AHE loops of Pd-seeded $[CoTaZr(0.5)/Pd(0.5)]_5$ samples after annealing at different temperatures for 1 h. (b) Coercivity versus CoTaZrlayer thickness for [CoTaZr/Pd] multilayers annealed at various temperatures. The field was applied along the easy magnetic axis (perpendicular to the film plane).

respectively. For the stacks with $t = 0.5$ nm, a degradation of the hysteresis squareness is observed for both sample series, which suggests that the in-plane volume anisotropy of the magnetic layer starts to gain over the perpendicular interfacial anisotropy. In the case of the Ta-seeded multilayer samples, no perpendicular anisotropy is found.

An improvement of the hysteresis squareness and an increase of the coercive field are observed for all Pd and Ru-seeded samples after annealing in vacuum at $T_a = 300\,^{\circ}C$ for 1 h. Figure 2(a) shows the normalized AHE loops at different T_a of a representative sample, a Pd-seeded $[CoTaZr(0.5)/Pd(0.5)]_5$ multilayer. Compared to the as-deposited stack, the remanent magnetization at zero field, M_r, for all annealed stacks is close to the saturation magnetization, M_s. The coercivity of the multilayer increases from 10 mT in the as-deposited state to 100 mT upon annealing at a temperature of 400 °C. Such an increase of the coercive field is accompanied, however, by a broadening of the magnetization switching field. The coercive fields of the $[CoTaZr/Pd]_5$ multilayers annealed at different temperatures are plotted in Figure 2(b) as a function of the CoTaZr thickness. Upon annealing, all Pd-seeded multilayers show a large increase of the coercive field, by almost a factor of 10 compared to as-deposited state. This is in contrast with the Ru-seeded samples, where the thermal annealing has little effect on the coercivity. We also notice that the Pd-seeded [CoTaZr(0.2)/Pd(0.5)]

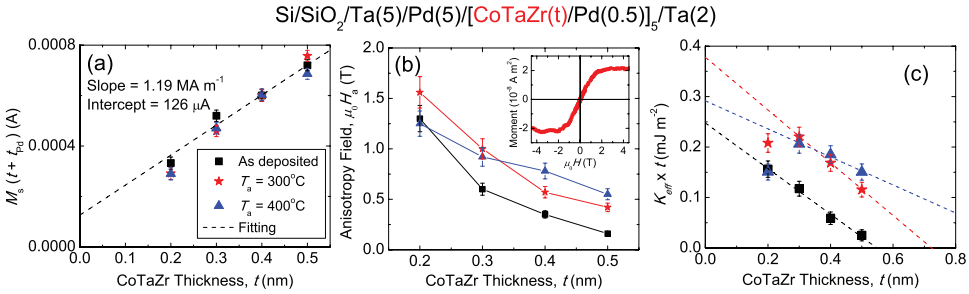

FIG. 3. (a) $M_s(t + t_{Pd})$ as a function of t for three series of multilayers. A linear fit is performed on data points for t ≥ 0.3 nm. The slope of the fitting is expected to be the saturation magnetization of the CoTaZr thin film. (b) Anisotropy field versus t for [CoTaZr/Pd] multilayers annealed at various temperatures. The field was applied along the hard magnetic axis (in the film plane). (Inset) SQUID magnetometry of [CoTaZr(0.2)/Pd(0.5)]$_5$ sample upon annealing at 300 °C for 1 h, showing the highest anisotropy field of ∼1.6 T. (c) $K_{\text{eff}}.t$ versus t for as-deposited and annealed multilayer samples. Dashed lines are linear fits to the data. Note that for the annealed sample series, the $t = 0.2$ nm data points deviate from the linear behaviour and are not considered for fitting.

stack experiences a decrease of coercive field when T_a is higher than 300 °C. This might be due to interdiffusion at higher T_a, to which the sample with the thinnest CoTaZr layer ($t = 0.2$ nm) is most vulnerable.

In the following paragraphs, we will focus on the properties of the Pd-seeded samples. We found a significant contribution of magnetically polarized Pd to the magnetization of the Pd-seeded [CoTaZr/Pd] multilayers, similar to that reported in [Co/Pd] system.[7,11] Using the approach suggested by Engel *et al.*,[11] we model the enhancement of the magnetization by the following equation:

$$M_s\,(t + t_{Pd}) = M_{s,CoTaZr}t + M_{s,Pd}t_{Pd}^{eff}\,, \tag{1}$$

where $M_s(t + t_{Pd})$ is calculated from the magnetic moment measured in SQUID divided by the area of the sample and the number of repeats in the multilayer ($N = 5$). $M_s(t + t_{Pd})$ for samples annealed at different T_a is plotted against t in Figure 3(a). Given that no significant change can be observed between the as-deposited and the annealed samples, we average the data for each CoTaZr thickness before performing a linear fit on data for t ≥ 0.3 nm. A positive intercept of the fitted line at $t = 0$ represents the interface-induced Pd polarization. Surprisingly, we found the slope of the fitted line to be 1.19 MA m^{-1}, markedly higher than the saturation magnetization measured using SQUID on a 1 μm thick film of CoTaZr, $M_s = 0.96$ MA m^{-1}. This discrepancy might suggest that in the limit of very thin multilayers, the induced Pd polarization increases slightly with increasing t. This can be understood by the fact that the ultrathin CoTaZr layer is not fully continuous, which allows a direct contact between the underneath and the top Pd through pin holes and gives rise to a lower induced polarization in Pd. Furthermore, the data points for $t = 0.2$ nm samples (not used for linear fitting) are well below the fitted line, reflecting a reduced Pd polarization in those samples compared to the thicker multilayers.

The in-plane anisotropy field, $\mu_0 H_a$, and the effective uniaxial anisotropy constant, K_{eff}, are the figures of merit for perpendicularly magnetized system. The thermal stability, Δ, of a tiny magnetic storage element of volume V is defined by $\Delta = \frac{K_{\text{eff}} V}{k_B T}$. To achieve 10 years data retention, the condition $\Delta > 60$ has to be satisfied. For example, a memory element such as the free layer of a magnetoresistive nanopillar of volume 10 nm × 10 nm × 3 nm has to be made of materials having the K_{eff} greater than 0.8 MJ m^{-3}. The magnitude of K_{eff} is determined from the area enclosed between the perpendicular and the in-plane M-H loops in the first quadrant, whereas the sign of K_{eff} reflects the magnetic easy axis direction.[1] In our convention, a positive (negative) K_{eff} implies an out-of-plane (in-plane) anisotropy. Note that in the Stoner-Wohlfarth limit, K_{eff} of a uniaxial ferromagnet is reduced to the area of a triangle with M_s in length and $\mu_0 H_a$ in width ($|K_{eff}| = (1/2)\mu_0 M_s H_a$), which is widely employed for the estimation of K_{eff}. Figure 3(b) is a plot of $\mu_0 H_a$ versus t for multilayers annealed at different T_a. For a given T_a, $\mu_0 H_a$ decreases with increasing t. This is primarily due to the competition between the in-plane volume anisotropy and the normal-to-plane interfacial anisotropy.

TABLE I. Summary of anisotropy parameters from data in Figure 3(c).

Annealing temperature, T_a (°C)	Volume anisotropy, K_v (MJ m^{-3})	Interface anisotropy, K_s (mJ m^{-2})	Effective anisotropy for $t = 0.2$ nm, K_{eff} (MJ m^{-3})
As-deposited	−0.45	0.12	0.98
300	−0.52	0.19	1.07
400	−0.28	0.15	0.77

It is worthy to note that the highest value of $\mu_0 H_a = 1.6$ T is measured on a [CoTaZr(0.2)/Pd(0.5)]$_5$ multilayer sample annealed at 300 °C (inset of Figure 3(b)). This corresponds to $K_{eff} = 1.1$ MJ m^{-3}. Upon annealing at a higher temperature ($T_a = 400$ °C), the sample still exhibits strong PMA with a lower anisotropy field of 1.2 T. This indicates the outstanding thermal annealing stability of the system, comparable with the ultrathin Co/Pd and Co/Pt multilayers reported in Ref. 14.

The K_{eff} can be phenomenologically decomposed into a volume (K_v) and an interfacial anisotropy (K_s) contribution by the following equation:

$$K_{eff}.t = K_V.t + 2K_s. \quad (2)$$

The factor of two in front of K_s takes into account the top CoTaZr/Pd and the bottom Pd/CoTaZr interfaces. Figure 3(c) plots $K_{eff}.t$ versus t for as-deposited and annealed multilayers. Linear fits of each data set are summarized in Table I. Upon annealing at 300 °C for 1 h, both the K_v and the K_s of the multilayer increase, compared to as-deposited state. We found the volume anisotropy after annealing at 300 °C of our sample ($K_{v,300} = -0.52$ MJ m^{-3}) to be similar to the evaporated Co/Pd (111) system ($K_v = -0.5$ MJ m^{-3}),[11] although the amorphous CoTaZr is used in our study, instead of the pure Co. If K_v were only due to shape anisotropy, from $|K_V| = |K_{shape}| = (1/2)\mu_0 M_s^2$, the calculated M_s is 0.91 MA m^{-1}. There is however a large difference in K_s between the one reported in Ref. 11 ($K_s = 0.63$ mJ m^{-2}), and our result ($K_{s,300} = 0.19$ mJ m^{-2}), which might be primarily due to the difference in Pd thickness (0.5 nm in our case and 1.0 nm in Ref. 11), and the dissimilar anisotropy between Co/Pd and CoTaZr/Pd interfaces. A further increase of T_a to 400 °C results in a decrease of K_v and the K_s. We interpret this as a consequence of intermixing between the magnetic and the non-magnetic species at high T_a.

While the fcc-textured [Co/Pd] multilayers are known to exhibit strong PMA, it is ambiguous in the case of [CoTaZr/Pd] multilayers because of the amorphous nature of relatively thick CoTaZr films. It is questionable that the ultrathin CoTaZr could be properly held to be amorphous in such multilayer stacks. To compare the structural properties of the [CoTaZr/Pd] multilayer with the well-studied [Co/Pd] system, we have grown two series of samples consist of Si/SiO$_2$ substrate/Ta(5)/Pd(5)/[Co/Pd or CoTaZr/Pd]$_{30}$/Ta(2), where the thicknesses of the magnetic (Co or CoTaZr) and non-magnetic (Pd) layers are 0.2 nm and 0.5 nm or 0.5 nm and 0.8 nm. The 2θ-θ X-ray diffraction scans are shown in Figure 4(a). For all samples, a main diffraction peak is observed between the bulk fcc-Pd(111) and Co(111) peaks. It mostly reflects a coherent Co(alloy)/Pd stack that adopts an intermediate interplanar distance. The left shoulder of the peak that coincides with the Pd(111) peak is mainly due to the unstrained Pd seed layer. For both samples with 0.5 nm thick Co and CoTaZr layers, a weak peak appears at $2\theta \approx 34°$, which may correspond to hcp-Co(0004). This could indicate the presence of a crystalline secondary phase with a texture similar to hcp-Co, regardless whether the Co or the CoTaZr alloy is used in the multilayer. Compared to Co-based multilayers, the main diffraction peak of the CoTaZr-based multilayers shifts towards the Pd(111) peak. This suggests that the use of CoTaZr reduces the stress within the stack due to the lattice mismatch between the Pd and the Co. The grazing incidence X-ray reflectivity scans (open squares) and fittings (lines) are plotted in Figure 4(b). We obtained reasonably good fits by considering the multilayer stack as a single, thick layer in the model. This fitting model is justified by the fact that the roughness found is comparable with individual layer thicknesses in the multilayers. Manifested by a faster attenuation of oscillations, the [Co(0.5)/Pd(0.8)]$_{30}$ multilayer is considerably rougher (roughness ≈ 1.1 nm) than the three other samples (roughness ≈ 0.7 nm). A higher strain/stress

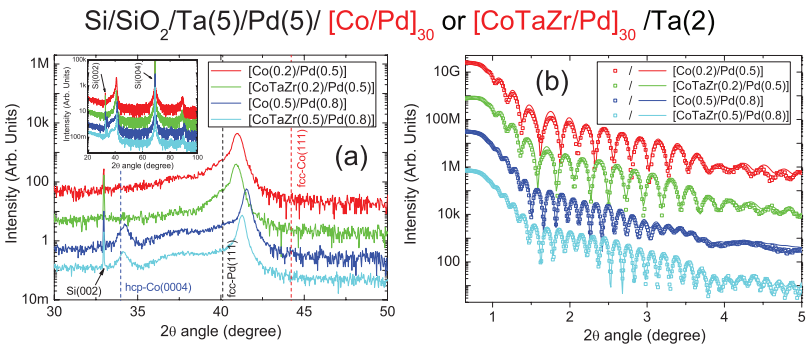

FIG. 4. (a) X-ray diffraction of $[Co/Pd]_{30}$ and $[CoTaZr/Pd]_{30}$ multilayers. The bulk fcc Pd(111) peak and the fcc Co(111) peaks are shown in dashed lines. (Inset) The full 2θ-θ scan which shows the (004) Si substrate peak. (b) Grazing incidence X-ray reflectivity scans. The measured data points and the best fitting curves are plotted in open squares and lines, respectively.

within the stack compared to the CoTaZr-based sample can potentially induce more dislocations and stacking faults, which can lead to a higher roughness.

In conclusion, the perpendicular magnetic anisotropy in [CoTaZr/Pd] multilayers is largely an interface effect, conditioned by the seed layer. Strong PMA is found on multilayers grown on Pd and Ru seed layers but not on Ta. The best Pd-seeded multilayer exhibits an effective perpendicular anisotropy constant, K_{eff} as high as 1.1 MJ m^{-3} after annealing at 300 °C. Although the very thin CoTaZr and Pd layers in the multilayer stacks will have intermixed to some extent, the presence of Pd is essential for the perpendicular anisotropy. Even though the CoTaZr layers may not be properly sustained in an amorphous state, the use of that alloy helps to reduce the stress within the multilayer while providing a smoother film. Since the PMA of the multilayer is maintained upon annealing at 400 °C for 1 h, the system is compatible with the CMOS processing.

The authors would like to thank Dr. Munuswamy Venkatesan for assistance on SQUID measurements and Dr. Karsten Rode for helpful discussions. This research was supported by Science Foundation Ireland (SFI) as part of the NISE project (Contract No. 10/IN1.13006).

[1] M. T. Johnson, P. J. H. Bloemen, F. J. A. Den Broeder, and J. J. De Vries, Rep. Prog. Phys. **59**, 1409–1458 (1996).
[2] B. D. Terris and T. Thomson, J. Phys. D **38**, R199–R222 (2005).
[3] S. Mangin, D. Ravelosona, J. A. Katine, M. J. Carey, B. D. Terris, and E. E. Fullerton, Nature Mater. **5**, 210–215 (2006).
[4] S. Yuasa and D. D. Djayaprawira, J. Phys. D **40**, R337–R354 (2007).
[5] K. Mizunuma, S. Ikeda, J. H. Park, H. Yamamoto, H. Gan, K. Miura, H. Hasegawa, J. Hayakawa, F. Matsukura, and H. Ohno, Appl. Phys. Lett. **95**, 232516 (2009).
[6] S. Bandiera, R. C. Sousa, M. M. De Castro, C. Ducruet, C. Portemont, S. Auffret, L. Vila, I. L. Prejbeanu, B. Rodmacq, and B. Dieny, Appl. Phys. Lett. **99**, 202507 (2011).
[7] P. F. Carcia, A. D. Meinhaldt, and A. Suna, Appl. Phys. Lett. **47**, 178–180 (1985).
[8] P. F. Carcia, J. Appl. Phys. **63**, 5066–5073 (1988).
[9] G. H. O. Daalderop, P. J. Kelly, and F. J. A. den Broeder, Phys. Rev. Lett. **68**, 682–685 (1992).
[10] F. J. A. den Broeder, D. Kuiper, A. P. van de Mosselaer, and W. Hoving, Phys. Rev. Lett. **60**, 2769–2772 (1988).
[11] B. N. Engel, C. D. England, R. A. Van Leeuwen, M. H. Wiedmann, and C. M. Falco, Phys. Rev. Lett. **67**, 1910–1913 (1991).
[12] P. F. Carcia, Z. G. Li, and W. B. Zeper, J. Magn. Magn. Mater. **121**, 452–460 (1993).
[13] O. Hellwig, T. Hauet, T. Thomson, E. Dobisz, J. D. Risner-Jamtgaard, D. Yaney, B. D. Terris, and E. E. Fullerton, Appl. Phys. Lett. **95**, 232505 (2009).
[14] K. Yakushiji, T. Saruya, H. Kubota, A. Fukushima, T. Nagahama, S. Yuasa, and K. Ando, Appl. Phys. Lett. **97**, 232508 (2010).
[15] H. Kurt, M. Venkatesan, and J. M. D. Coey, J. Appl. Phys. **108**, 073916 (2010).
[16] C. Fowley, N. Decorde, K. Oguz, K. Rode, H. Kurt, and J. M. D. Coey, IEEE Trans. Magn. **46**, 2116–2118 (2010).
[17] A. M. Crawford, D. Gardner, and S. X. Wang, IEEE Trans. Magn. **38**, 3168–3170 (2002).
[18] E. M. T. Velu, S. Malhotra, G. Bertero, and D. Wachenschwanz, IEEE Trans. Magn. **39**, 668–672 (2003).
[19] H. S. Jung, E. M. T. Velu, S. S. Malhotra, W. Jiang, and G. Bertero, J. Appl. Phys. **99**, 08E702 (2006).
[20] D. W. Lee and S. X. Wang, J. Appl. Phys. **103**, 07E907 (2008).